TÜBİTAK

Turkish Journal of Chemistry

http://journals.tubitak.gov.tr/chem/

Research Article

Turk J Chem
(2013) 37: 119 – 133

doi:10.3906/kim-1204-8

Molecular docking and QSAR study on imidazole derivatives as 14α-demethylase inhibitors

Asghar DAVOOD[1,*], **Maryam IMAN**[2]

[1]Department of Medicinal Chemistry, Pharmaceutical Sciences Branch, Islamic Azad University, Tehran, Iran

[2]Chemical Injuries Research Center, Baqiyatallah University of Medical Sciences, Tehran, Iran

Received: 04.04.2012 • **Accepted:** 04.12.2012 • **Published Online:** 24.01.2013 • **Printed:** 25.02.2013

Abstract: 14α-Demethylase (CYP51) inhibitors have been widely used in the treatment of fungal infections. In this study, a series of imidazole derivatives with CYP51 inhibitory activity were subjected to a molecular docking study followed by quantitative structure–activity relationship (QSAR) analyses in search of the ideal physicochemical characteristics of potential CYP51 inhibitors. Desired imidazoles were built using the HyperChem program, and conformational studies were performed through a semiempirical method followed by the PM3 method. Docking study was performed using the AutoDock program on all of the compounds.

Different QSAR descriptors were calculated using DRAGON, AutoDock, and HyperChem. Multilinear regression was used as a chemometric tool for QSAR modeling. The docking study indicated that all of compounds **1**–**43** interact with the 14α-demethylase, and azole–heme coordination and $\pi - \pi$ and π-cation interactions are involved in drug–receptor interaction. In the $\pi - \pi$ and π-cation interactions, the aryl moieties interact with Phe 255 and Arg 96, and the role of the phenoxy group is more important than that of the phenyl group.

The developed QSAR model indicated the importance of atomic van der Waals volumes and atomic Sanderson electronegativities. The sums of the R6u, RDF030v, Mor25v, GATs5e, and R5e+ were identified as the most significant descriptors. The developed QSAR model was statistically significant according to the validation parameters.

Key words: Antifungal, azole, docking, imidazole, QSAR

1. Introduction

Research and development of potent and effective antimicrobial agents represents one of the most important advances in therapeutics, not only in the control of serious infections, but also in the prevention and treatment of some infectious complications of other therapeutic modalities such as cancer chemotherapy and surgery. Over the past decade, fungal infection became an important complication and a major cause of morbidity and mortality in immunocompromised individuals, such as those suffering from tuberculosis, cancer, or AIDS, and in organ transplant cases.[1] In these hosts with impaired immune systems, the fungal pathogens can easily invade into the tissues and cause serious infections with higher rates of morbidity and mortality.[2,3] *Candida albicans*, *Cryptococcus neoformans*, and *Aspergillus fumigatus* were the most common causes of invasive fungal infections.[4,5] In the clinic, antifungal agents that can be used for life-threatening fungal infections are limited. These drugs fall into 5 major classes: azoles, allylamines, polyenes, fluoropyrimidines, and thiocarbamates.[6]

*Correspondence: adavood@iaups.ac.ir

Among them, azoles are the most widely used antifungal agents because of their high therapeutic index.

The azoles are a large and relatively new group of synthetic compounds, of which imidazoles and triazoles are 2 clinically useful families employed in the treatment of systemic fungal infections as well as in agriculture.[7–9] Azole antifungal agents inhibit the cytochrome P450 sterol 14α-demethylase (14DM, CYP51) by a mechanism in which the heterocyclic nitrogen atom (N-3 of imidazole and N-4 of triazole) binds to the heme iron atom in the binding site of the enzyme. Lanosterol-14α-demethylase (CYP51) is one of the key enzymes of sterol biosynthesis in fungi.[10] The resulting ergosterol depletion and the accumulation of precursor 14α-methylated sterols disrupt the structure of the plasma membrane, making it more vulnerable to further damage, and alter the activities of several membrane-bound enzymes.[11,12] The efficacy of azoles depends on the strength of the binding to heme iron as well as the affinity of the N-1 substituent for the protein of the cytochrome.[13] Because of the existence of CYP51 in fungi as well as in mammals, azole antifungal agents are generally toxic.[14,15] The selective inhibition of P450 14DM results in the reduction of the biosynthesis of ergosterol, thus causing accumulation of lanosterol and 14-methylsterols and subsequent growth inhibition.[13] Recently, it has been reported that the azole antifungal drugs have effects on CYP3A4 as well as multidrug-resistant protein 1 (MDR1).[16] However, the extensive use of azoles has led to the development of severe resistance,[17,18] which greatly reduced their efficacy. This situation has led to an ongoing search for new azoles.

Discovery of new agents against *Candida albicans* that were designed by replacing the methylamino terminus of fluoxetine (Figure 1a) with the imidazole ring have been reported recently.[19] The new imidazole showed potent antifungal activity superior to that of miconazole (Figure 1b) and other drugs of clinical interest, and 1-[3-(2,4-dichlorophenoxy)-3-(4-chlorophenyl)propyl]-1*H*-imidazole (Figure 1c) was found to be the most potent tested compound. To develop structure–activity relationships (SARs) studies, the lead structure was

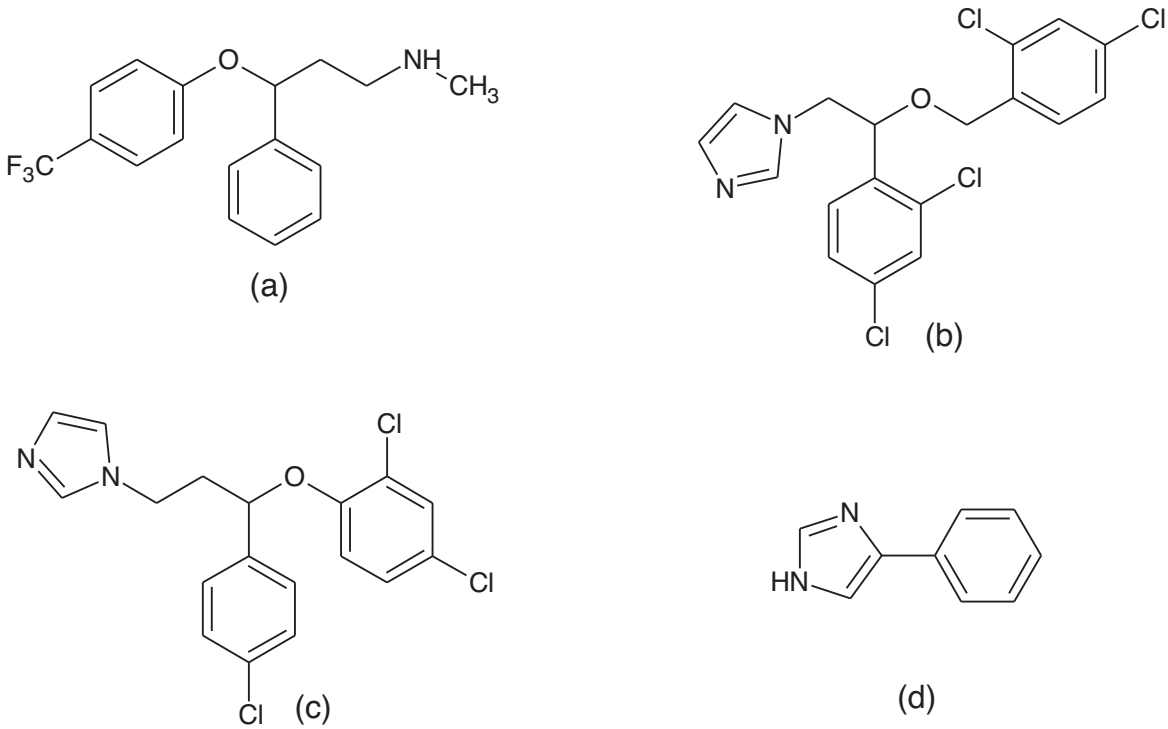

Figure 1. Structures of fluoxetine (a), miconazole (b), 1-[3-(2,4-dichlorophenoxy)-3-(4-chlorophenyl)propyl]-1*H*-imidazole (c), and 4-phenylimidazole (d).

dissected into 4 sections: (A) the imidazole ring, (B) the phenyl ring, (C) the phenoxy group, and (D) the alkyl chain (Figure 2). Using this model, some new derivatives were designed and synthesized (Table 1).[20]

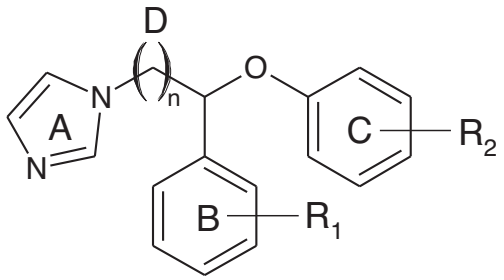

Figure 2. The dissected structure of lead compound into 4 parts: A) the imidazole ring, B) the phenyl ring, C) the phenoxy group, and D) the alkyl chain.

The reported results[21−30] demonstrated the power of combining docking and quantitative SAR (QSAR) approaches to explore the probable binding conformations of compounds at the active sites of the protein target, and further provided useful information in understanding the structural and chemical features of ligands and lead compounds in designing and finding new potential inhibitors. Progressive docking, a hybrid QSAR/docking approach was used to accelerating in silico high throughput screening[31]

Herein we used the combined molecular docking and QSAR approach to model the antifungal activity of imidazole derivatives. In this study, a series of imidazole derivatives that were evaluated as antifungal agents[20] were subjected to a molecular docking study followed by QSAR analyses in search of the ideal physicochemical characteristics of potential azoles

2. Experimental

2.1. Molecular modeling and docking: software and method

2.1.1. Software

The chemical structure of the desired azoles (Table 1) was built using HyperChem software (version 7, Hypercube Inc.). Conformational analysis of the compounds was performed through the semiempirical molecular orbital calculation (PM3) method by using the HyperChem software. Total energy gradient was calculated as a root mean square (RMS) value, until the RMS gradient was 0.01 kcal mol^{-1}. The gradient (G) is the rate of change (first derivative) of total energy (E) with respect to displacement of each atom in the x, y, and z directions for atoms from 1 to n. The HyperChem package reports this value for geometry optimization and single point calculations. An RMS gradient of zero means that the structure is at a local minimum or saddle point in the potential energy surface, not necessarily at the structure and state of the lowest energy (global minimum). Among all the energy minima conformers, the global minima of compounds were used in docking calculations, and the resulting geometry was transferred into the AutoDock (version 4.2) program package, which was developed by Arthur J. Olson Chemometrics Group.[32] The docking calculations were performed using AutoDockTools (ADT). Crystal structures of cytochrome P450 14α-sterol demethylase (CYP51) (to 2.10-A resolution) were downloaded from the PDB bank server (PDB entry 1E9X).[33] In the lanosterol-14α-demethylase that was downloaded from the PDB bank server, some amino acid side chain atoms are missing. A reconstruction of the whole side chain was attempted using Swiss PDB viewer 4.0.1.

Table 1. The chemical structure of azoles **1**–**43**.

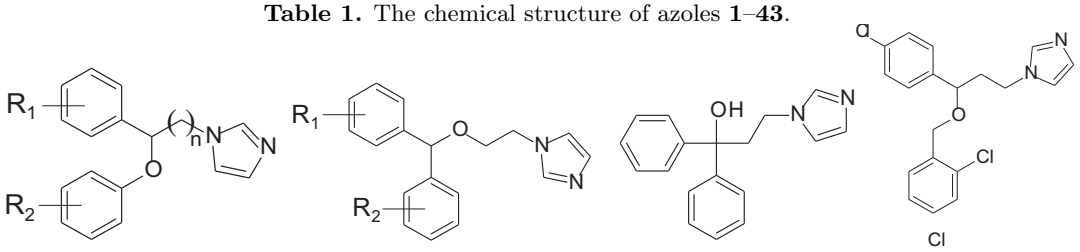

1-38 39-41 42 43

Compd.	R_1	R_2	n	MIC	Compd.	R_1	R_2	n	MIC
1	H	H	2	62.7	**24**	4-Me	4-Cl	2	2.4
2	H	4-Cl	2	3.3	**25**	4-Me	4-Me	2	4
3	H	4-Me	2	10.2	**26**	4-Me	4-Et	2	8.7
4	H	2,4-Cl_2	2	6.07	**27**	4-Me	4-i-Pr	2	16.6
5	H	2,6-Cl_2	2	46.2	**28**	4-Me	4-t-Bu	2	52.1
6	H	3,5-Cl_2	2	13.8	**29**	4-Me	2,4-Cl_2	2	3.15
7	4-Cl	H	2	8.8	**30**	4-Me	2,6-Cl_2	2	42
8	4-Cl	2-Cl	2	7.7	**31**	4-Me	3,5-Cl_2	2	11.9
9	4-Cl	4-Cl	2	5.5	**32**	4-Me	2-Cl,4-Me	2	6.5
10	4-Cl	4-Me	2	3.2	**33**	4-Me	4-Cl,2-Me	2	16
11	4-Cl	4-Et	2	6.5	**34**	4-Me	2,4-Me_2	2	46.5
12	4-Cl	4-i-Pr	2	18.5	**35**	2,4-Cl_2	2,4-Cl_2	2	51
13	4-Cl	4-t-Bu	2	57.1	**36**	4-Cl	4-Me	1	22.3
14	4-Cl	2,4-Cl_2	2	2.85	**37**	4-Cl	4-Me	3	2.1
15	4-Cl	2,6-Cl_2	2	5	**38**	4-Cl	4-Me	4	32
16	4-Cl	3,5-Cl_2	2	7.7	**39**	H	H		78.1
17	4-Cl	2,4-Me_2	2	13.5	**40**	2,4-Cl_2	H		46.1
18	4-F	H	2	32.1	**41**	2,4-Cl_2	4-Cl		34.35
19	4-F	4-Me	2	7	**42**				114
20	4-F	2,4-Cl_2	2	2.9	**43**				60.2
21	4-F	2,6-Cl_2	2	36.1	Mic				3.25
22	4-F	3,5-Cl_2	2	8.8	Eco				4.3
23	4-Me	H	2	20.3	Flu				15.3

Mic: miconazole, Eco: econazole, Flu: fluoxetine.

2.1.2. Method

Docking studies were carried out using AutoDock 4.2. This program starts with a ligand molecule in an arbitrary conformation, orientation, and position and finds favorable dockings in a protein-binding site using both simulated annealing and genetic algorithms. The ADT, which has been released as an extension suite to the Python Molecular Viewer, was used to prepare the protein and the ligand. For the macromolecule, the crystal structure of lanosterol-14α-demethylase and polar hydrogen were added, and then Kollman United Atom charges and atomic solvation parameters were assigned. The grid maps of docking studies were computed using the AutoGrid4.2 included in the AutoDock 4.2 distribution. The grid center that was centered on the active site was obtained by trial and error and previous study,[33] and 65, 65, 65 points with grid spacing of 0.375 were calculated. The GA-LS method was adopted to be defined as follows: a maximum number of 2,500,000 energy evaluations; a maximum number of generations of 27,000; and mutation and crossover rates of 0.02 and 0.8, respectively. Pseudo-Solis and Wets parameters were used for local search, and 300 iterations of Solis and Wets local search were imposed. The number of docking runs was set to 50. Both AutoGrid and AutoDock

computations were performed on Cygwin. After docking, all structures generated were assigned to clusters based on a tolerance of 1 Å all-atom RMS deviation from the lowest energy structure.

Hydrogen bonding and hydrophobic interactions between docked potent agents and macromolecules were analyzed using ADT (version 1.50). The best docking result can be considered to be the conformation with the lowest (docked) energy. In order to assign our docking methods and parameters, we docked the 4-phenylimidazole (Figure 1d), a compound that acts as a lanosterol-14α-demethylase inhibitor, into the active site of lanosterol-14α-demethylase and compared it with the crystalline structure of lanosterol-14α-demethylase that was inactivated by 4-phenylimidazole (1E9X).[33]

2.2. Computation of structural descriptors and QSAR equations

2.2.1. Software

The resulting geometry of optimized azoles **1**–**43** (Table 1) was transferred into the DRAGON program package, which was developed by Milano Chemometrics and the QSAR Group.[34] MATLAB (version 7.6.0., R2008a) and SPSS (version 18) were used for the multilinear regression (MLR) method.

2.2.2. Data set and descriptor generation

The biological data used in this study are the anti-*Candida albicans* activities as minimum inhibition concentrations (MICs) from a set of 43 azole derivatives (Table 1)[20] that were used for subsequent QSAR analysis as dependent variables. A large number of molecular descriptors were calculated using AutoDock (Table 2), HyperChem (Table 3), and the DRAGON package. Some chemical parameters including molecular volume (V), molecular surface area (SA approx), surface area (SA grid) hydrophobicity (LogP), hydration energy (HE), refractivity (Rf), molecular polarizability (MP), and different quantum chemical descriptors including dipole moment (DM) and HOMO energies were calculated using HyperChem (Table 3). DRAGON software was used to calculate different functional groups (topological, geometrical, and constitutional descriptors) for each molecule. Results based on the docked conformations (Table 2) are the intermolecular energy, Vdw-hb-desolv energy, electrostatic energy, total internal energy, torsional energy, unbound energy, predicted binding energy, and inhibition constant (Ki), which we used as descriptors in QSAR studies.

2.2.3. Data screening and model building

The calculated descriptors were first analyzed for the existence of constant or near-constant variables, and those detected were removed. In addition, to decrease the redundancy existing in the descriptor data matrix, the correlation of descriptors with each other and with the activity (MIC) of the molecules was examined and collinear descriptors (i.e. $r > 0.9$) were detected. Among the collinear descriptors, the one that had the highest correlation with activity was retained and the others were removed from the data matrix. The calculated descriptors were collected in a data matrix whose number of rows and columns were the number of molecules and descriptors, respectively. To select the set of descriptors that were most relevant to the percentage of antifungal activity, the MLR models were built and the QSAR equations with stepwise selection and elimination of variables were established by the MLR method.

Table 2. Docking results of azoles **1**–**43** using AutoDock 4.2 software.

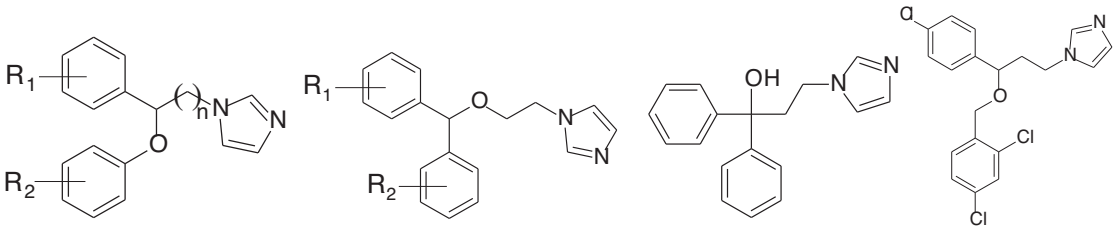

1-38 39-41 42 43

No.	[a] BE	[b] LE	[c] IC	[d] IE	[e] VE	[f] EE	[g] TI	[h] TE	[i] UE	LogP	MIC
1	–6.98	–0.33	7.6	–8.77	–8.76	–0.01	–0.95	1.79	–0.95	3.98	62.7
2	–7.98	–0.36	1.41	–9.77	–9.82	0.05	–0.81	1.79	–0.81	4.50	3.3
3	–7.97	–0.36	1.43	–9.76	–9.77	0.0	–0.92	1.79	–0.92	4.45	10.2
4	–7.26	–0.32	4.73	–9.05	–9.03	–0.02	–0.54	1.79	–0.54	5.02	6.07
5	–8.24	–0.36	909.53	–10.03	–10.01	–0.03	–0.09	1.79	–0.09	5.02	46.2
6	–8.38	–0.36	717.04	–10.17	–10.24	–0.07	–0.27	1.79	–0.27	5.02	13.8
7	–8.12	–0.37	1.11	–9.91	–9.9	–0.01	–0.02	1.79	–0.02	4.50	8.8
8	–8.44	–0.37	651.98	–10.23	–10.26	0.03	0.29	1.79	0.29	5.02	7.7
9	–8.9	–0.39	300.04	–10.69	–10.71	0.02	–0.43	1.79	–0.43	5.02	5.5
10	–8.98	–0.39	260.45	–10.77	–10.75	–0.02	0.31	1.79	0.31	4.96	3.2
11	–8.85	–0.37	327.46	–10.93	–10.96	0.03	–0.44	2.09	–0.44	5.36	6.5
12	–9.59	–0.38	93.9	–11.68	–11.72	0.05	–0.61	2.09	–0.61	5.69	18.5
13	–9.68	–0.37	80.38	–11.77	–11.84	0.08	–0.46	2.09	–0.46	6.12	57.1
14	–9.16	–0.38	193.01	–10.95	–11	0.05	–0.67	1.79	–0.67	5.53	2.85
15	–8.51	–0.35	578.85	–10.3	–10.41	0.11	–0.85	1.79	–0.85	5.53	5
16	–8.88	–0.37	308.25	–10.67	–10.65	–0.02	–0.47	1.79	–0.47	5.53	7.7
17	–8.24	–0.34	914.06	–10.03	–10.02	–0.01	–0.66	1.79	–0.66	5.43	13.5
18	–7.7	–0.35	2.27	–9.49	–9.57	0.08	–0.86	1.79	–0.86	4.12	32.1
19	–7.86	–0.34	1.73	–9.65	–9.71	0.06	–0.65	1.79	–0.65	4.59	7
20	–8.17	–0.34	1.03	–9.96	–10.02	0.06	–0.8	1.79	–0.8	5.15	2.9
21	–7.78	–0.32	1.99	–9.57	–9.58	0.02	0.45	1.79	0.45	5.15	36.1
22	–7.84	–0.33	1.8	–9.63	–9.65	0.02	–0.27	1.79	–0.27	5.69	8.8
23	–8.09	–0.37	1.17	–9.88	–9.9	0.02	–0.6	1.79	–0.6	4.45	20.3
24	–8.36	–0.36	755.19	–10.14	–10.13	–0.01	–0.32	1.79	–0.32	4.96	2.4
25	–8(8)	–0.35	1.36	–9.79	–9.84	0.04	–0.81	1.79	–0.81	4.91	4
26	–8.61	–0.36	492.38	–10.69	–10.66	–0.04	–0.22	2.09	–0.22	5.31	8.7
27	–8.54	–0.34	551.19	–10.63	–10.62	–0.01	–0.22	2.09	–0.22	5.64	16.6
28	–9.83	–0.38	61.88	–11.92	–11.94	0.02	–0.89	2.09	–0.89	6.07	52.1
29	–8.94	–0.37	281.24	–10.73	–10.8	0.08	–0.81	1.79	–0.81	5.48	3.15
30	–8.34	–0.35	767.44	–10.13	–10.14	0.01	–0.15	1.79	–0.15	5.48	42
31	–8.73	–0.36	401.13	–10.52	–10.54	0.02	0.19	1.79	0.19	5.48	11.9
32	–8.7	–0.36	421.09	–10.49	–10.54	0.05	–0.63	1.79	–0.63	5.43	6.5
33	–8.71	–0.36	415.54	–10.5	–10.55	0.06	–0.63	1.79	–0.63	5.43	16
34	–8.61	–0.36	486.41	–10.4	–10.42	0.01	–0.44	1.79	–0.44	5.38	46.5
35	–8.97	–0.36	265.74	–10.76	–10.83	0.07	–0.49	1.79	–0.49	6.05	51
36	–8.53	–0.39	558.66	–10.02	–10.02	0	–0.88	1.49	–0.88	4.91	22.3

Table 2. Contunied.

No.	[a] BE	[b] LE	[c] IC	[d] IE	[e] VE	[f] EE	[g] TI	[h] TE	[i] UE	LogP	MIC
37	–9.19	–0.38	182.87	–11.28	–11.26	–0.02	–1.11	2.09	–1.11	5.42	2.1
38	–7.71	–0.31	2.23	–10.1	–10.05	–0.05	–0.8	2.39	–0.8	5.81	32
39	–6.85	–0.33	9.6	–8.64	–8.67	0.03	–1.36	1.79	–1.36	3.92	78.1
40	–7.72	–0.34	2.19	–9.51	–9.55	0.04	–1.37	1.79	–1.37	4.96	46.1
41	–7.9	–0.33	1.63	–9.69	–9.58	–0.11	–0.58	1.79	–0.58	5.48	34.35
42	–7.96	–0.38	1.46	–9.75	–9.7	–0.05	–0.46	1.79	–0.46	3.43	114
43	–9.35	–0.37	138.91	–11.44	–11.41	–0.03	–0.42	2.09	–0.42	5.53	60.2
Mic	–9.26	–0.37	163.8	–11.05	–11.08	0.03	–1.1	1.79	–1.1	5.99	3.25
Eco	–8.96	–0.37	271.76	–10.75	–10.82	0.07	–1.13	1.79	–1.13	5.48	4.3

[a]BE = binding energy (kcal/mol), [b]LE = ligand efficiency, [c]IC = inhibition constant (nM),
[d]IE = intermolecular energy, [e]VE = Vdw-hb-desolv energy, [f]EE = electrostatic energy,
[g]TI = total internal, [h]TE = torsional energy, [i]UE =unbound energy. Mic: miconazole, Eco: econazole.

3. Results and discussion

3.1. Molecular modeling and docking

Docking calculations were performed using AutoDock and a reconstruction of the whole side chain of the lanosterol-14α-demethylase attempted using Swiss PDB viewer 4.0.1. In order to assign the perfect grid of each ligand, grid box values were obtained and docking was performed using the implemented Lamarckin GL (genetic algorithm and local search combination) with 10 independent docking runs for each azole. Flexible docking of all data sets used for the computational study was carried out on the active site of 14α-demethylase. Docking scores showed that these compounds docked to the active site of the enzyme comparable to 4-phenylimidazole and miconazole. The predicted binding energy and other results of docking of these inhibitors into the active site are listed in Table 2. The predicted binding energy is the sum of the intermolecular energy and the torsional free-energy penalty by which both of them can affect the mode of interaction of azoles with the enzyme 14-DM. The semiempirical free energy force field that was used by AutoDock to evaluate conformation during docking simulation includes 6 pairwise evaluations (V) and an estimate of the conformational entropy lost upon binding (Sconf):

$$\Delta G = (\bigvee_{bound}^{L-L} - \bigvee_{unbound}^{L-L}) + (\bigvee_{bound}^{P-P} - \bigvee_{unbound}^{P-P}) + (\bigvee_{bound}^{P-L} - \bigvee_{unbound}^{P-L} + \Delta S_{conf}),$$

where L refers to the ligand and P refers to the protein in a ligand–protein docking calculation. Each of the pairwise energetic terms includes evaluations for dispersion/repulsion, hydrogen bonding, electrostatics, and desolvation by which all of them can be affected by changing the substituent in the azoles. There is a good and acceptable relation between predicted binding energy and MIC, and some of compounds had very good docking energy, but in the biological study those were not more active and this may be dependent on their low LogP.

Our drug–receptor interaction studies reveal that all of compounds **1**–**43** interact with the 14α-demethylase by azole–heme coordination and $\pi-\pi$ and π-cation interactions. In some of them, there is an additional hydrogen binding interaction. The heterocyclic nitrogen atom, N-3 of imidazole, binds to the heme iron atom in the binding site of the enzyme (Figure 3). In some of azoles there are 2 interactions with heme (Figure 4). In the $\pi-\pi$ and π-cation interactions, the aryl moieties phenyl and phenoxy, or both of them, interact with Phe 255 and Arg 96, respectively. In the $\pi-\pi$ and π-cation interactions the role of the phenoxy group is more important than that of the phenyl group (Figure 5). In compound **20**, the phenoxy moiety has 2 $\pi-\pi$ interaction

Table 3. Calculated properties of azoles using the HyperChem software.

Comp.	HOMO	[a]DM	[b]SA	[c]SA	[d]V	[e]HE	LogP	[f]R	[g]P
1	–9.393179	4.578	438.75	532.01	882.53	–6.83	3.98	83.58	33.19
2	–9.138861	4.218	474.16	558.49	928.17	–6.49	4.50	88.38	35.11
3	–9.079765	4.735	481.43	559.76	931.19	–5.65	4.45	88.62	35.02
4	–9.26808	4.51	499.66	574.65	961.49	–5.87	5.02	93.19	37.04
5	–9.352364	5.307	456.39	547.74	937.52	–6.02	5.02	93.19	37.04
6	–9.415345	3.872	508.72	588.41	973.91	–6.12	5.02	93.19	37.04
7	–9.374125	4.633	479.08	561.02	932.58	–6.33	4.50	88.38	35.11
8	–9.286543	4.692	502.63	580.03	968.71	–5.87	5.02	93.19	37.04
9	–9.188782	3.883	513.62	583.18	974.27	–6	5.02	93.19	37.04
10	–9.382726	4.762	512.71	585.12	978.94	–5.30	4.96	93.42	36.95
11	–9.156409	4.601	547.22	618.97	1029.16	–4.70	5.36	98.03	38.78
12	–9.319655	4.643	578.53	637.61	1069.90	–4.38	5.69	102.57	40.62
13	–9.370285	5.429	602.09	638.92	1109.69	–4.05	6.12	107.05	42.45
14	–9.189535	3.991	542.66	606.41	1011.94	–5.58	5.53	97.99	38.97
15	–9.367484	5.454	498.31	578.24	988.05	–5.65	5.53	97.99	38.97
16	–9.450666	3.792	537.93	605.45	1008.03	–5.76	5.53	97.99	38.97
17	–9.360182	4.558	531.62	595.73	1011.89	–4.40	5.43	98.47	38.78
18	–9.420826	3.591	456.73	544.55	895.84	–6.59	4.12	83.79	33.09
19	–9.145886	3.939	492.20	567.27	937.77	–5.34	4.59	88.84	34.93
20	–9.160608	4.04	514.01	586.59	976.34	–5.67	5.15	93.40	36.95
21	–9.35671	5.4	476.76	563.16	951.32	–5.64	5.15	93.40	36.95
22	–9.319655	4.643	578.53	637.61	1069.90	–4.38	5.69	102.57	40.62
23	–9.357091	4.811	489.61	563.88	940.18	–5.70	4.45	88.62	35.02
24	–9.14677	4.557	520.78	584.71	979.55	–5.35	4.96	93.42	36.95
25	–9.274726	5.008	533.21	590.86	994.38	–4.49	4.91	93.66	36.86
26	–9.053041	5.451	552.37	625.26	1037.14	–3.87	5.31	98.26	38.69
27	–9.147958	5.101	586.40	639.06	1078.03	–3.55	5.64	102.81	40.53
28	–9.133238	6.112	569.09	633.86	1094.52	–1.94	6.07	107.29	42.36
29	–9.229021	5.323	544.56	604.21	1014.43	–4.66	5.48	98.23	38.88
30	–9.298559	5.777	521.05	586.05	994.79	–4.72	5.48	98.23	38.88
31	–9.435598	4.501	555.67	611.17	1011.82	–5.00	5.48	98.23	38.88
32	–9.32783	6.136	540.89	593.70	1007.49	–4.16	5.43	98.47	38.78
33	–9.072541	3.98	543.69	598.67	1016.41	–4.04	5.43	98.47	38.78
34	–8.954204	4.708	552.98	610.54	1027.14	–3.32	5.38	98.70	38.69
35	–9.186337	3.673	563.05	618.56	1043.55	–5.34	6.05	102.80	40.90
36	–9.160514	3.88	478.21	556.78	926.10	–5.05	4.91	88.56	35.11
37	–9.090929	4.097	532.24	611.91	1024.83	–4.69	5.42	98.07	38.78
38	–9.264651	3.851	589.68	645.47	1085.23	–4.76	5.81	102.67	40.62
39	–9.43484	4.054	426.35	531.73	883.65	–6.26	3.92	83.82	33.19
40	–9.40124	3.295	467.85	560.92	948.34	–5.54	4.96	93.43	37.04
41	–9.435816	3.509	519.23	589.29	992.99	–5.32	5.48	98.23	38.97
42	–9.262797	4.564	372.16	495.47	846.14	–7.31	3.43	83.82	33.19
43	–9.407544	2.799	540.84	606.04	1036.47	–4.73	5.53	103.10	40.81

[a]DM = dipole moment, [b]SA = surface area (approx), [c]SA = surface area (grid),
[d]V = volume, [e]HE = hydration energy, [f]R = refractivity, [g]P = polarizability.

with Phe 255 and Phe 83 (Figure 6), and in compound **37**, phenoxy interacts with Phe 78 by $\pi - \pi$ interaction (Figure 7). In compounds **39**, **40**, **41**, **42**, and **43** there is no azole–heme interaction, and in compounds **41**

and **42**, the nitrogen of azole makes a hydrogen bond with Arg 96 (Figure 8). In compounds **8** and **22**, there is additional hydrogen binding between azole and Thr 260. These results reveals that the position of phenyl and phenoxy moieties and the type and position of substituent on the aryl ring strongly affect the orientation of the azole ring and subsequently the interaction of N-3 of imidazole with the heme iron atom in the binding site of the enzyme.

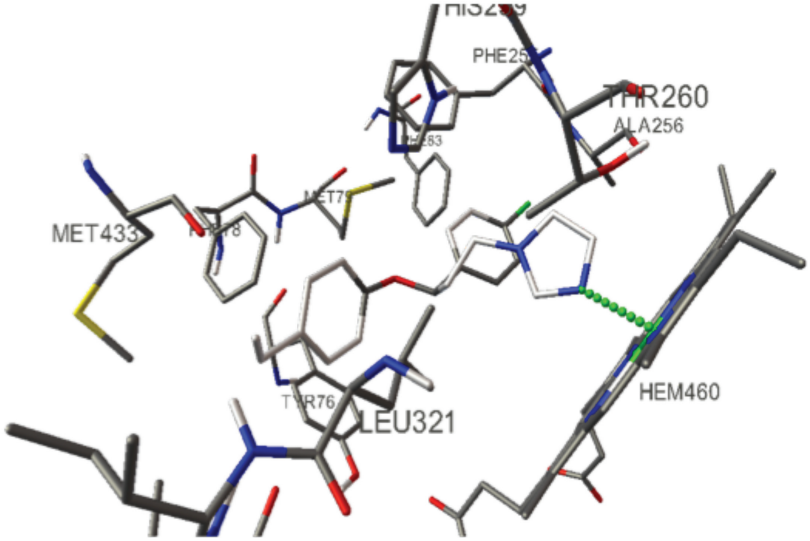

Figure 3. Docked structures of compound **11** in the model of 14-DM; azoles are displayed as sticks and the N-3 of imidazole–heme coordination is represented with dashed green lines. Docking study done by using ADT program and 14-DM model obtained from PDB server.

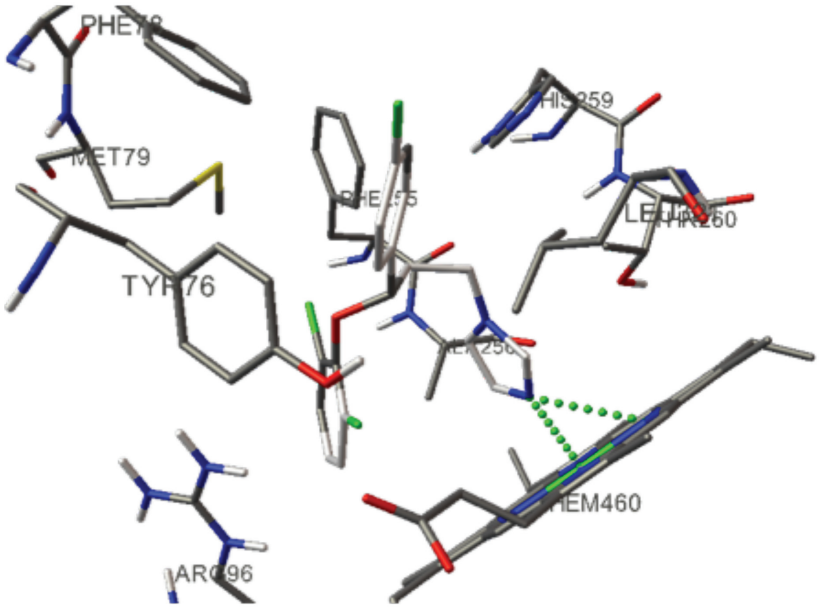

Figure 4. Docked structures of compound **15** in model of 14-DM; azoles are displayed as sticks and the N-3 of imidazole–heme coordination is represented with dashed green lines. Docking study done by using ADT program and 14-DM model obtained from PDB server.

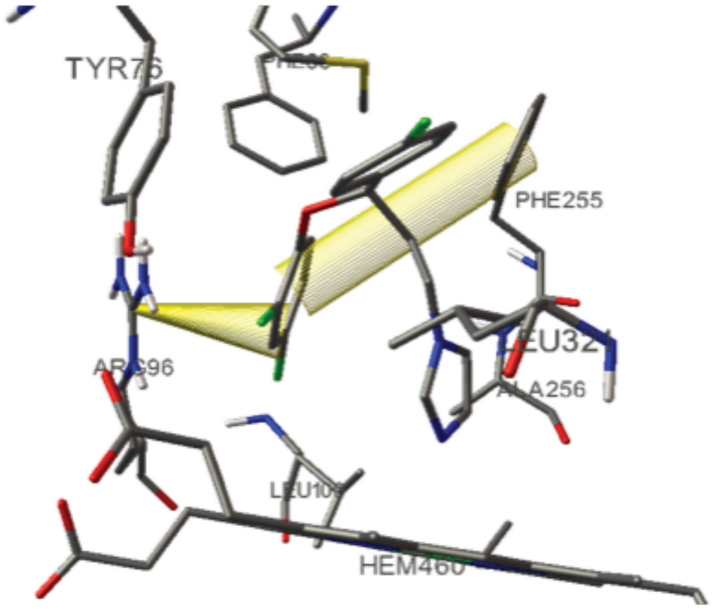

Figure 5. Docked structures of compound **14** in model of 14-DM; azoles are displayed as sticks and the $\pi - \pi$ and π-cation interactions with Phe 255 and Arg 96 are represented with yellow cylinders. Docking study done by using ADT program and 14-DM model obtained from PDB server.

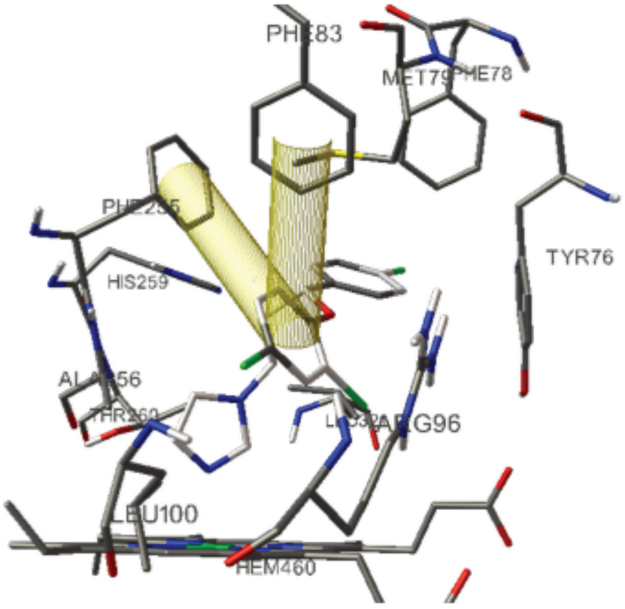

Figure 6. Docked structures of compound **20** in model of 14-DM; azoles are displayed as sticks and the $\pi - \pi$ interactions with Phe 255 and Phe 83 are represented with yellow cylinders. Docking study done by using ADT program and 14-DM model obtained from PDB server.

3.2. QSAR equations

Based on the procedure explained in the experimental section, by using a stepwise multiple linear regression method, the following 5-parametric equation was derived for azoles **1**–**43**. The correlation coefficient matrix for the descriptors used in the MLR equation is shown in Table 4.

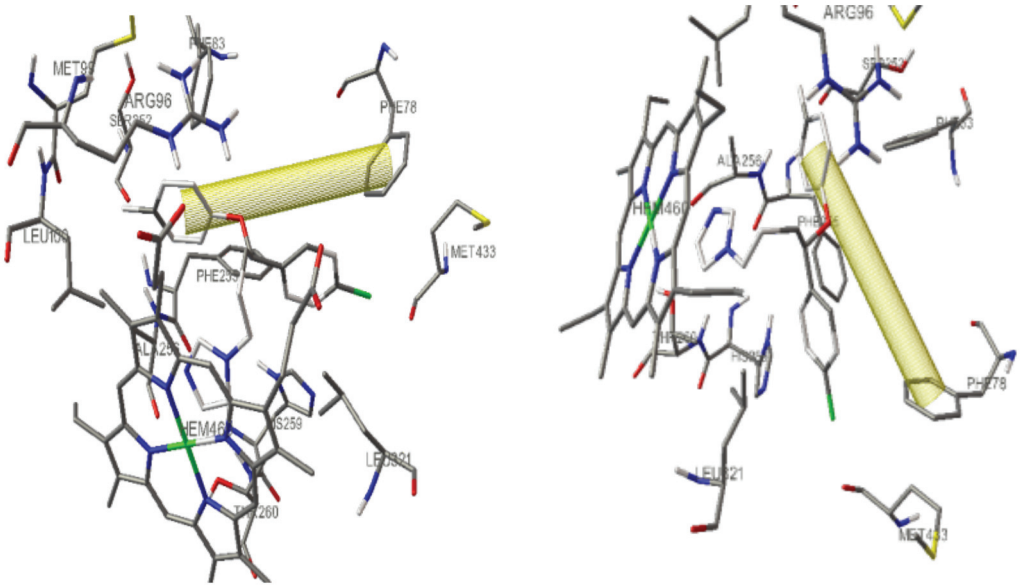

Figure 7. Docked structures of compound **37** in model of 14-DM; azoles are displayed as sticks and the $\pi-\pi$ interactions of phenoxy with Phe 78 are represented with yellow cylinders. Docking study done by using ADT program and 14-DM model obtained from PDB server.

Eq. (1) could explain 94% of the variance in MIC data and the relative error prediction (REP) of this equation is shown in Table 5. This equation describes the effect of 2-dimensional (GATS5e) and 3-dimensional (R6u, RDF030v, Mor25v, and R5e+) indices on antifungal activity.

Table 4. Correlation coefficient matrix for the descriptors used in MLR equation.

Correlations							
		R6u	RDF030v	Mor25v	GATS5e	R5e+	MIC
R6u	Pearson correlation	1	0.115	-0.310	0.268	0.687	0.600
	Sig. (2-tailed)		0.464	0.043	0.083	0.000	0.000
	N	43	43	43	43	43	43
RDF030v	Pearson correlation	0.115	1	–0.219	0.176	0.173	0.413
	Sig. (2-tailed)	0.464		0.159	0.258	0.267	0.006
	N	43	43	43	43	43	43
Mor25v	Pearson correlation	–0.310	–0.219	1	–0.098	–0.299	–0.064
	Sig. (2-tailed)	0.043	0.159		0.534	0.052	0.685
	N	43	43	43	43	43	43
GATS5e	Pearson correlation	0.268	0.176	–0.098	1	0.115	0.531
	Sig. (2-tailed)	0.083	0.258	0.534		0.464	0.000
	N	43	43	43	43	43	43
R5e+	Pearson correlation	0.687	0.173	–0.299	0.115	1	0.521
	Sig. (2-tailed)	0.000	0.267	0.052	0.464		0.000
	N	43	43	43	43	43	43
MIC	Pearson correlation	0.600	0.413	–0.064	0.531	0.521	1
	Sig. (2-tailed)	0.000	0.006	0.685	0.000	0.000	
	N	43	43	43	43	43	43

Table 5. Antifungal activity of azoles **1**–**43**.

Comp.	[a]MIC $_{Exp.}$	[b]MIC $_{Pred.}$	[c]|REP|
1	62.7	48.84	0.283
2	3.3	5.23	0.369
3*	10.2	16.35	0.376
4	6.07	3.75	0.618
5	46.2	49.26	0.062
6	13.8	21.17	0.348
7	8.8	7.84	0.122
8	7.7	10.37	0.257
9	5.5	5.54	0.007
10	3.2	28.25	0.886
11*	6.5	18.04	0.639
12	18.5	15.6	0.185
13	57.1	38.99	0.464
14	2.85	3.51	0.188
15	5	38.44	0.869
16*	7.7	25.3	0.695
17	13.5	48.93	0.724
18	32.1	7.1	3.521
19	7	6.64	0.054
20*	2.9	5.06	0.426
21*	36.1	28.23	0.278
22	8.8	2.6	2.384
23	20.3	28.07	0.276
24	2.4	3.2	0.250
25*	4	12.83	0.688
26	8.7	43.78	0.801
27	16.6	24.42	0.320
28	52.1	45.11	0.154
29	3.15	2.92	0.078
30	42	35.3	0.189
31	11.9	12.86	0.074
32	6.5	10.56	0.384
33*	16	6.71	1.384
34*	46.5	37.25	0.248
35	51	54.49	0.064
36*	22.3	24.54	0.091
37	2.1	3.45	0.391
38	32	26.83	0.192
39	78.1	73.71	0.059
40	46.1	50.1	0.079
41	34.35	26.08	0.317
42	114	113.32	0.006
43*	60.2	54.35	0.107

[a]MIC in *Candida albicans*, [b]the calculated MIC by using multilinear regression Eq. (1), [c]absolute relative error of prediction, *compounds used as prediction set.

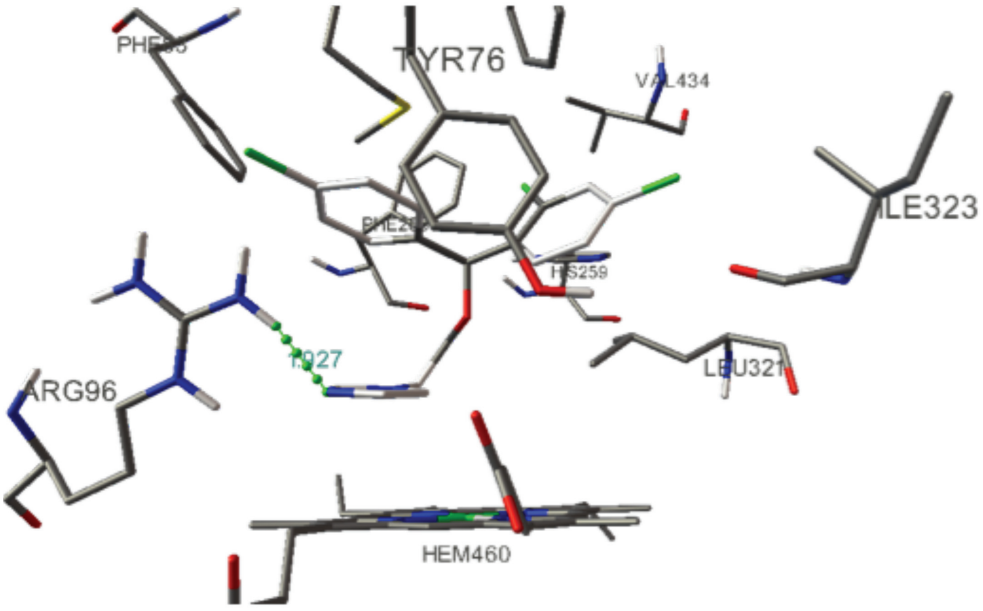

Figure 8. Docked structures of compound **41** in model of 14-DM; azoles are displayed as sticks and the hydrogen binding with Phe Arg96 is represented with dashed green lines. Docking study done by using ADT program and 14-DM model obtained from PDB server.

$$MIC = -294.282 + 66.138(R6u) + 13.076(RDF030v) + 135.986(Mor25v) + 32.770(GATs5e) + 391.628(R5e+) \quad (1)$$

$$n = 43, F = 18.33, R^2 = 0.940, P < 0.0001, q^2 = 0.70$$

R6u and R5e+ belong to 3D GETAWAY descriptors, and R6u is unweighted and R5e+ is weighted by atomic Sanderson electronegativities. RDF030v and Mor25v belong to RDF and 3D-MoRSE descriptors, respectively, weighted by atomic van der Waals volumes. GATS5e corresponds to Geary autocorrelation, one of the 2D autocorrelations, and is weighted by atomic Sanderson electronegativities.

Eq. (1) reveals that electronegativity and van der Waals volumes of the substituent strongly affect the biological response. Indices R5e+ and GATs5e represent the importance of electronegativity and indices Mor25v and RDF030v represent the importance of van der Waals volumes. Descriptors R5e+ and Mor25v with coefficients 391.628 and 135.986 mainly affected the antifungal activity of these types of azoles.

4. Conclusions

In the docking studies, we confirmed that all of compounds **1**–**43** interact with the 14α-demethylase, and azole–heme coordination and $\pi-\pi$ and π-cation interactions are involved in the drug–receptor interaction. Based on the molecular modeling studies, the position of aryl and the type and position of substituent on the aryl ring strongly affect the orientation and interaction of imidazole with the receptor. The phenoxy group plays a more important role in the $\pi-\pi$ and π-cation interactions.

Based on the QSAR studies, electronegativity and van der Waals volumes of the substituent strongly affect the biological response. Indices R5e+ and Mor25v with coefficients 391.628 and 135.986 have the main effect on the antifungal activity of these types of azoles.

These observations and experimental results provide a good process for explanation of the potent and selective inhibitory activity of these compounds. These computational studies can offer some useful references for understanding the action mechanism and performing the molecular design or modification of this series of 14α-demethylase inhibitors.

Acknowledgment

We thank Professor Arthur J. Olson for his kindness in offering us the AutoDock 4.2 program. Technical assistance of the Medicinal Chemistry Department of Azad University in performing the computational studies is gratefully acknowledged.

References

1. Rostom, S. A.; Ashour, H. M.; El Razik, H. A.; El Fattah Ael, F.; El-Din, N. N. *Bioorg. Med. Chem.* **2009**, *17*, 2410–2422.
2. Minari, A.; Husni, R.; Avery, R. K.; Longworth, D. L.; DeCamp, M.; Bertin, M.; Schilz, R.; Smedira, N.; Haug, M. T.; Mehta, A.; Gordon, S. M. *Transpl. Infect. Dis.* **2002**, *4*, 195–200.
3. Edmond, M. B.; Wallace, S. E.; McClish, D. K.; Pfaller, M. A.; Jones, R. N.; Wenzel, R. P. *Clin. Infect. Dis.* **1999**, *29*, 239–244.
4. Steenbergen, J. N.; Casadevall, A. *J. Clin. Microbiol.* **2000**, *38*, 1974–1976.
5. Latge, J. P. *Clin. Microbiol. Rev.* **1999**, *12*, 310–350.
6. De Luca, L. *Curr. Med. Chem.* **2006**, *13*, 1–23.
7. Zhu, J.; Lu, J.; Zhou, Y.; Li, Y.; Cheng, J.; Zheng, C. *Bioorg. Med. Chem. Lett.* **2006**, *16*, 5285–5289.
8. Roberts, T. R.; Hutson, D. *Metabolic Pathways of Agrochemicals. Part 2: Insecticides and Fungicides*, Royal Society of Chemistry, Cambridge, 1999.
9. Sheehan, D. J.; Hitchcock, C. A.; Sibley, C. M. *Clin. Microbiol. Rev.* **1999**, *12*, 40–79.
10. Vanden Bossche, H.; Koymans, L. *Mycoses* **1998**, *41*, 32–38.
11. Georgopapadakou, N. H.; Walsh, T. J. *Antimicrob. Agents Chemother.* **1996**, *40*, 279–291.
12. Lupetti, A.; Danesi, R.; Campa, M.; Tacca, M. D.; Kelly, S. *Trends Mol. Med.* **2002**, *8*, 76–81.
13. Weinberg, E. D. In *Burger's Medicinal Chemistry and Drug Discovery*; Abraham, D. J., Ed.; John Wiley & Sons, New York, 1996.
14. Slama, J. T.; Hancock, J. L.; Rho, T.; Sambucetti, L.; Bachmann, K. A. *Biochem. Pharmacol.* **1998**, *55*, 1881–1892.
15. Wulff, H.; Miller, M. J.; Hansel, W.; Grissmer, S.; Cahalan, M. D.; Chandy, K. G. *Proc. Nat. Acad. Sci. USA* **2000**, *97*, 8151–8156.
16. Sakaeda, T.; Iwaki, K.; Kakumoto, M.; Nishikawa, M.; Niwa, T.; Jin, J.; Nakamura, T.; Nishiguchi, K.; Okamura, N.; Okumura, K. *J. Pharm. Pharmacol.* **2005**, *57*, 759–764.
17. Hoffman, H. L.; Ernst, E. J.; Klepser, M. E. *Expert Opin. Invest. Drugs* **2000**, *9*, 593-605.
18. Casalinuovo, I. A.; Di Francesco, P.; Garaci, E. *Eur. Rev. Med. Pharmacol. Sci.* **2004**, *8*, 69.
19. Silvestri, R.; Artico, M.; La Regina, G.; Di Pasquali, A.; De Martino, G.; D'Auria, F. D.; Nencion, L.; Palarmara, A. T. *J. Med. Chem.* **2004**, *47*, 3924–3926.
20. La Regina, G.; D'Auria, F. D.; Tafi, A.; Piscitelli, F.; Olla, S.; Caporuscio, F.; Nencioni, L.; Cirilli, R.; La Torre, F.; De Melo, N. R.; Kelly, S. L.; Lamb, D. C.; Artico, M.; Botta, M.; Palamara, A. T.; Silestri, R. *J. Med. Chem.* **2008**, *51*, 3841–3855.
21. Roy, P. P.; Roy, K. *J. Pharm. Pharmacol.* **2010**, *62*, 1717–1728.

22. Dai, Y.; Wang, Q.; Zhang, X.; Jia, S.; Zheng, H.; Feng, D. *Eur. J. Med. Chem.* **2010**, *45*, 5612–5620.

23. Saíz-Urra, L.; Pérez, M. A. C.; Helguera, A. M.; Froeyen, M. *Eur. J .Med. Chem.* **2011**, *46*, 2736–2747.

24. Davood, A.; Nematollahi, A.; Iman, M.; Shafiee, A. *Med. Chem. Res.* **2010**, *19*, 58-70.

25. Davood, A.; Iman, M. *Med. Chem. Res.* **2011**, *20*, 955–961.

26. Nematollahi, A; Davood, A. *Int. J. Chem.Tech Res.* **2010**, *2* 1808–1815.

27. Iman, M.; Davood, A.; Nematollahi, A.; Dehpoor, A. R.; Shafiee, A. *Arch. Pharm. Res.* **2011**, *34*, 1417–1426.

28. Masanda, V. H; Mahajana, D. T; Patila, K. N; Padoleb, N; Haddac, T. B; Alafeefyd, A. A. *J. Comput. Method. Mol. Design* **2011**, *1*, 49–56.

29. Pana, X.; Tana, N.; Zenga, G.; Hana, H.; Huanga, H *Bioorg. Med. Chem.* **2006**, *14*, 2771–2778.

30. Wang, Q.; Mach, R. H.; Reichert, D. E. *J. Chem. Inf. Model.* **2009**, *49* 1963–1973.

31. Cherkasov, A.; Ban, F.; Li, Y.; Fallahi, M *J. Med. Chem.* **2006**, *49*, 7466–7478.

32. Morris, G. M.; Goodsell, D. S.; Pique, M. E.; Lindstrom, W. L.; Huey, R.; Forli, S.; Hart, W. E.; Halliday, S.; Belew, R.; Olson, A. J. AutoDock 4.2 with AutoDockTools. http://autodock.scripps.edu/faqs-help/manual/autodock-4-2-user-guide/AutoDock4.2_UserGuide.pdf, 2009.

33. Podust, L. M.; Poulos, T. L.; Waterman, M. R. *Proc. Natl. Acad. Sci.* **2001**, *98*, 3068.

34. Todeschini, R. Milano Chemometrics and QSAR Group, http://michem.disat.unimib.it/, e-dragon (http://www.vcclab.org/ lab/edragon), 2008.